Analysis of Fracture Probabilities in Nonuniformly Stressed Brittle Materials

by N. A. WEIL and I. M. DANIEL

IIT Research Institute, Chicago, Illinois

The results of theoretical studies on the effect of nonuniform stress fields encountered in prismatic beams under bending on the fracture of brittle materials are described. Derivations were carried out to determine the risk of rupture of bending specimens subjected to a symmetrical four-point load of arbitrary spacing, the symmetric three-point loading and pure bending forming limiting cases of this more general loading. The analysis was based on materials obeying the Weibull distribution function with assumptions for either volumetric or surface flaw dispersion conditions. The predicted strengths of bending and tensile specimens are compared. An analytical method for the determination of the three Weibull parameters from a pure bending test is proposed. This method, based on the best fit of a theoretical curve to the experimental data, was applied successfully to experimental results on Columbia Resin, a brittle amorphous polymer.

I. Introduction

IN PRACTICAL applications ceramic parts are almost invariably subjected to loading conditions resulting in nonuniform internal stresses. In fact, because of the purely elastic nature of these substances, it is difficult to impose uniform stresses on them even under the most carefully controlled conditions. In most laboratory tests, bodies are therefore subjected to some form of nonuniform stress.

In recent years there has been an increased awareness that the fracture strength of ceramic substances can be satisfactorily represented only as a statistical quantity, and suitable approaches have been developed to extend this statistical treatment to bodies subjected to nonuniform stresses. In all these theories, however, it has been assumed that the cumulative fracture probability for the entire body is determined by summing the probability of fracture of its infinitesimal component elements, each subjected to a uniform state of stress. It has been assumed that a stress gradient and the shear stresses that inevitably accompany it do not contribute to failure by themselves.

To date no attempt has been made to confirm the validity of this assumption. An investigation was therefore undertaken to examine the influence of the nonuniformity of stress on the probability of fracture and to determine whether the existence of a stress gradient, per se, had a demonstrable effect on the fracture strength. This investigation was carried out in two complementary parts, namely, an analytical program and an experimental program.

The results of theoretical studies concerning the influence of nonuniform stress fields on the fracture characteristics of brittle materials are presented here. The complementary experimental program was completed after this paper was submitted and the results were presented recently.[1]

The most widely accepted statistical theory of fracture is based on the Weibull distribution function.[2] Two basic criteria of fracture, size and normal stress, are used, and it is postulated that failure in an isotropic, homogeneous material is fully described by three material parameters: the zero strength, the flaw density exponent, and a scale parameter. Within the validity of these assumptions, the theory can describe failure for any type of stress distribution, uniform or nonuniform, uniaxial or polyaxial. For these reasons, the Weibull theory was selected as the basis of the analytical work described here.

Analyses of fracture probabilities in the presence of a stress gradient have been conducted by Weibull himself and more recently by Weiss *et al.*[3] Although nonlinear gradients were investigated, the simplifying assumption of a zero value for the zero strength was made.

The nonuniform stress field chosen for the present analysis was that of the simple beam subjected to four-point loading. This stress field is one of the simplest nonuniform stress fields that can be studied; in fact, for pure bending a single parameter, the stress gradient, is sufficient to describe the stress distribution. This specimen shape and loading condition also lends itself excellently to carefully controlled tests and was used for all the experimental work in this program.

Basic to any experimental work on the effect of a given parameter is the need for obtaining a completely reliable fundamental statistical distribution of strengths for the material in question. Customarily, such is done either by the trial-and-error graphical method originally suggested by Weibull or by analytical approaches devised by others.[4]

Presented at the Sixty-Fifth Annual Meeting, The American Ceramic Society, Pittsburgh, Pa., April 30, 1963 (Symposium on Mechanical Properties of Ceramics, No. 1–1s–63). Received May 16, 1963; revised copy received December 12, 1963.

This research was supported by the Aeronautical Systems Division (ASD), Air Force Systems Command, Wright-Patterson Air Force Base, Ohio, under Contract No. AF33(616)–7465.

At the time this work was done, the writers were, respectively, director, Mechanics Research Division, and research engineer, Experimental Stress Analysis Section, IIT Research Institute (formerly Armour Research Foundation). N. A. Weil is now vice-president of research, Cummins Engine Company, Inc., Columbus, Indiana.

[1] I. M. Daniel and N. A. Weil, "Influence of Stress Gradient Upon Fracture of Brittle Materials," ASME Paper 63–WA–228; presented at Winter Annual Meeting, American Society of Mechanical Engineers, Philadelphia, Pa., November 17–22, 1963.

[2] (*a*) W. Weibull, "Statistical Theory of Strength of Materials," *Ing. Vetenskaps Akad. Handl.*, No. 151, 45 pp. (1939); *Ceram. Abstr.*, **19** [3] 78 (1940).

(*b*) W. Weibull, "Phenomenon of Rupture in Solids," *Ing. Vetenskaps Akad. Handl.*, No. 153, 55 pp. (1939); *Ceram. Abstr.*, **20** [10] 250 (1941).

(*c*) W. Weibull, "Statistical Distribution Function of Wide Applicability," *J. Appl. Mech.*, **18** [3] 293 (September 1951).

[3] (*a*) V. Weiss, J. G. Sessler, and K. S. Grewal, "Effect of Stress Gradient and Stress Biaxiality on Behavior of Materials," ASD–TR–61–725 (1961).

(*b*) V. Weiss, J. Sessler, K. Grewal, and R. Chait, "Effect of Stress Concentration on Fracture and Deformation Characteristics of Ceramics and Metals," ASD–TDR–63–380, 58 pp. (April 1963).

[4] (*a*) F. A. McClintock, discussion of footnote 2(*c*) above, *J. Appl. Mech.*, **19** [2] 233 (June 1952).

(*b*) O. K. Salmassy, E. G. Bodine, W. H. Duckworth, and G. K. Manning, "Behavior of Brittle-State Materials," Wright Air Development Center Technical Report No. 53–50, 164 pp. (September 1954).

(*c*) Waloddi Weibull, "Statistical Evaluation of Data from Fatigue and Creep-Rupture Tests: I, Fundamental Concepts

The graphical method cannot be freed, however, from errors attributable to subjective judgments, and the analytical treatments are mostly suitable for a large number of purely tensile specimens.

Therefore, following the theoretical derivations for the effect of nonuniform stress fields, an analytical method is presented here for defining the best fit of a theoretical Weibull curve to a set of experimentally obtained data. The appropriate parameters are obtained by a minimization process of the sum of the mean squares. The procedure thus developed is then demonstrated by applying it to a series of bending tests conducted on Columbia Resin (CR-39) specimens.

II. Weibull Theory

Two basic criteria of failure, size and normal tensile stress, are used in the Weibull theory. For a uniaxial stress field in a homogeneous isotropic material, governed by volumetric flaw distribution, the probability of fracture at a given stress σ is given by

$$S = \begin{cases} 1 - \exp\left[-\int_V \left(\frac{\sigma - \sigma_u}{\sigma_0}\right)^m dV\right] = 1 - e^{-B}, & \sigma \geqslant \sigma_u \\ 0, & \sigma < \sigma_u \end{cases} \tag{1}$$

where

$$B = \int_V \left(\frac{\sigma - \sigma_u}{\sigma_0}\right)^m dV \tag{2}$$

is the risk of rupture and

σ_u = zero probability strength (location parameter).
m = flaw density exponent (shape parameter).
σ_0 = scale parameter.

The last three parameters are associated with the material and are independent of size.

The mean failure stress is given by

$$\sigma_m = \sigma_u + \int_{\sigma_u}^{\infty} e^{-B} d\sigma \tag{3}$$

and the variance by

$$a^2 = \int_{\sigma_u}^{\infty} e^{-B} d(\sigma^2) + \sigma_u{}^2 - \sigma_m{}^2 \tag{4}$$

Equation (1) shows that the theory does not make any special allowance for the nonuniformity of stress distribution. Each infinitesimal element of a specimen is considered to be under uniform tensile stress, and the risk of rupture for the whole specimen is obtained by integrating the risk of rupture of each infinitesimal element over the volume of the specimen. The stress gradient does not enter as an independent parameter, and all the nonuniformity effects seem to be accounted for by the risk of rupture. The question of whether the stress gradient has an independent effect on the fracture stress is equivalent to the question of whether the Weibull theory is sufficient to predict failure for nonuniform stress fields.

In a material governed by surface flaw distribution the risk of rupture is given by

$$B = \int_A \left(\frac{\sigma - \sigma_u}{\sigma_0}\right)^m dA \tag{5}$$

To establish the dependence of the risk of rupture on the dimensions of a specimen and on the type of loading, the risk of rupture was calculated for the general case of a prismatic beam under four-point loading. Derivations were made for both volumetric and surface flaw distribution.

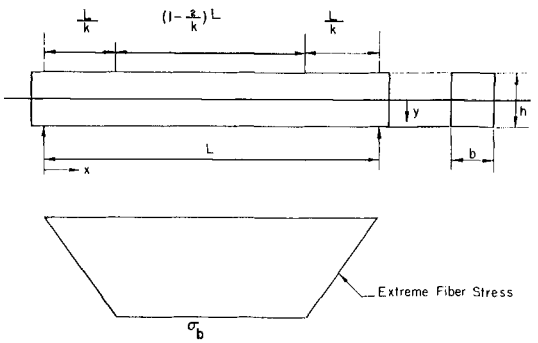

Fig. 1. Prismatic beam under four-point loading and distribution of extreme fiber stress.

III. Risk of Rupture

(1) Material Governed by Volumetric Flaw Distribution

The distribution of tensile stresses in the beam shown in Fig. 1 is

$$\begin{aligned} \sigma &= \frac{2k\sigma_b}{hL} yx \text{ for } 0 \leqslant x \leqslant \frac{L}{k} \text{ and } \left(1 - \frac{1}{k}\right) L \leqslant x \leqslant L \\ \sigma &= \frac{2\sigma_b}{h} y \text{ for } \frac{L}{k} \leqslant x \leqslant \left(1 - \frac{1}{k}\right) L \end{aligned} \tag{6}$$

The risk of rupture is then composed of two parts

$$B_b = B_b' + B_b'' \tag{7}$$

where B_b' corresponds to the central portion of the specimen subjected to uniform bending and B_b'' refers to the outer portions. It can be shown that

$$B_b' = \frac{V\left(1 - \frac{2}{k}\right)}{2(m+1)} \left(1 - \frac{\sigma_u}{\sigma_b}\right) \left(\frac{\sigma_b - \sigma_u}{\sigma_0}\right)^m \tag{8}$$

and

$$B_b'' = \frac{V}{2(m+1)} \left(1 - \frac{\sigma_u}{\sigma_b}\right) \left(\frac{\sigma_b - \sigma_u}{\sigma_0}\right)^m \frac{2}{k} \sum + \frac{V}{k(m+1)\sigma_b\sigma_0{}^m} (-\sigma_u)^{[m]+1} I_\alpha \tag{9}$$

where

$m = [m] + \alpha$, with $[m]$ the largest integer less than or equal to m.

$$I_\alpha = \int_{y_u}^{h/2} \frac{1}{y} \left(\frac{2\sigma_b}{h} y - \sigma_u\right)^\alpha dy \tag{10}$$

$$y_u = \frac{h}{2} \frac{\sigma_u}{\sigma_b}$$

$$\sum = \sum_{r=0}^{[m]} \frac{1}{m+1-r} \left(1 - \frac{\sigma_b}{\sigma_u}\right)^{-r} \tag{11}$$

Using equation (7) one obtains

$$B_b = \frac{V}{2(m+1)} \left(1 - \frac{\sigma_u}{\sigma_b}\right) \left(\frac{\sigma_b - \sigma_u}{\sigma_0}\right)^m \left(1 - \frac{2}{k} + \frac{2}{k} \sum\right) + \frac{V}{k(m+1)\sigma_b\sigma_0{}^m} (-\sigma_u)^{[m]+1} I_\alpha \tag{12}$$

If m is an integer, i.e., if $m = [m]$, then $\alpha = 0$ and equation (12) reduces to

$$B_b = \frac{V}{2(m+1)} \left(1 - \frac{\sigma_u}{\sigma_b}\right) \left(\frac{\sigma_b - \sigma_u}{\sigma_0}\right)^m \left(1 - \frac{2}{k} + \frac{2}{k} \sum\right) + \frac{V}{k(m+1)\sigma_b\sigma_0{}^m} (-\sigma_u)^{m+1} \ln \frac{h}{2y_u} \tag{13}$$

and General Methods," Wright Air Development Center Technical Report No. 59-400, 78 pp. (September 1959).

(*d*) I. M. Daniel and N. A. Weil, "Effect of Non-Uniform Stress Fields"; pp. 119-69 in Studies of Brittle Behavior of Ceramic Materials, Task 3, ASD-TR-61-628, 495 pp. (April 1962). N. A. Weil, editor.

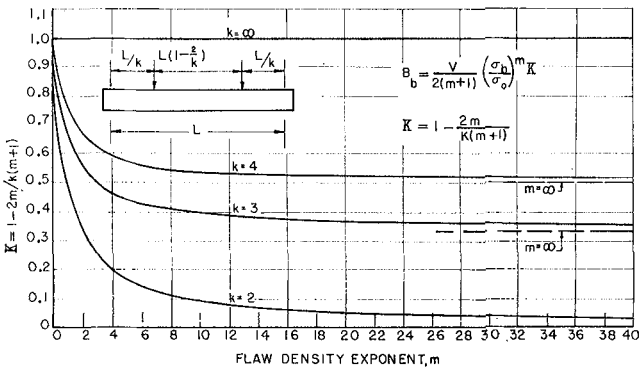

Fig. 2. Loading factor *K* vs. flaw density exponent *m* for material governed by volumetric flaw distribution.

Specific forms of this equation can be obtained by assigning values to the parameter k.

(*a*) *Pure bending* ($k = \infty$)

$$B_b = \frac{V}{2(m+1)}\left(1 - \frac{\sigma_u}{\sigma_b}\right)\left(\frac{\sigma_b - \sigma_u}{\sigma_0}\right)^m \tag{14}$$

(*b*) *Fourth-point loading* ($k = 4$)

$$B_b = \frac{V}{4(m+1)}\left(1 - \frac{\sigma_u}{\sigma_b}\right)\left(\frac{\sigma_b - \sigma_u}{\sigma_0}\right)^m (1 + \Sigma) + \frac{V}{4(m+1)\sigma_b\sigma_0{}^m}(-\sigma_u)^{m+1} \ln \frac{h}{2y_u} \tag{15}$$

(*c*) *Third-point loading* ($k = 3$)

$$B_b = \frac{V}{6(m+1)}\left(1 - \frac{\sigma_u}{\sigma_b}\right)\left(\frac{\sigma_b - \sigma_u}{\sigma_0}\right)^m (1 + 2\Sigma) + \frac{V}{3(m+1)\sigma_b\sigma_0{}^m}(-\sigma_u)^{m+1} \ln \frac{h}{2y_u} \tag{16}$$

(*d*) *Three-point loading (center-point loading;* $k = 2$)

$$B_b = \frac{V}{2(m+1)}\left(1 - \frac{\sigma_u}{\sigma_b}\right)\left(\frac{\sigma_b - \sigma_u}{\sigma_0}\right)^m \Sigma + \frac{V}{2(m+1)\sigma_b\sigma_0{}^m}(-\sigma_u)^{m+1} \ln \frac{h}{2y_u} \tag{17}$$

When $\sigma_u = 0$, both equations (12) and (13) reduce to

$$B_b = \frac{V}{2(m+1)}\left(\frac{\sigma_b}{\sigma_0}\right)^m \frac{k(m+1) - 2m}{k(m+1)} \tag{18}$$

Again, listed below are some typical cases of interest for specific values of k.

(*a*) *Pure bending* ($k = \infty$)

$$B_b = \frac{V}{2(m+1)}\left(\frac{\sigma_b}{\sigma_0}\right)^m \tag{19}$$

(*b*) *Fourth-point loading* ($k = 4$)

$$B_b = \frac{V}{4(m+1)}\left(\frac{\sigma_b}{\sigma_0}\right)^m \frac{m+2}{m+1} \tag{20}$$

(*c*) *Third-point loading* ($k = 3$)

$$B_b = \frac{V}{6(m+1)}\left(\frac{\sigma_b}{\sigma_0}\right)^m \frac{m+3}{m+1} \tag{21}$$

(*d*) *Three-point loading (center-point loading;* $k = 2$)

$$B_b = \frac{V}{2(m+1)}\left(\frac{\sigma_b}{\sigma_0}\right)^m \frac{1}{m+1} \tag{22}$$

The variation of the risk of rupture with the spacing of concentrated loads on the beam is described by the factor

$$K = \frac{k(m+1) - 2m}{k(m+1)} \tag{23}$$

in equation (18). The relation among the values of B_b given in equations (19) through (22) is illustrated in Fig. 2 by plotting the factor K versus the parameter m.

(2) Material Governed by Surface Flaw Distribution

For the stress distribution defined by equation (6) one has

$$B_b = \frac{L}{m+1}\left(1 - \frac{\sigma_u}{\sigma_b}\right)\left(\frac{\sigma_b - \sigma_u}{\sigma_0}\right)^m \left[\left(1 - \frac{2}{k}\right)h + \frac{2h}{k}\sum + \frac{2b}{k}\right] + \left(1 - \frac{2}{k}\right)\left(\frac{\sigma_b - \sigma_u}{\sigma_0}\right)^m Lb + \frac{2hL}{k(m+1)\sigma_b\sigma_0{}^m}(-\sigma_u)^{[m]+1} I_\alpha \tag{24}$$

If m is an integer, equation (24) reduces to

$$B_b = \frac{L}{m+1}\left(1 - \frac{\sigma_u}{\sigma_b}\right)\left(\frac{\sigma_b - \sigma_u}{\sigma_0}\right)^m \left[\left(1 - \frac{2}{k}\right)h + \frac{2h}{k}\sum + \frac{2b}{k}\right] + \frac{2hL}{k(m+1)\sigma_b\sigma_0{}^m}(-\sigma_u)^{m+1} \ln \frac{h}{2y_u} + \left(1 - \frac{2}{k}\right)\left(\frac{\sigma_b - \sigma_u}{\sigma_0}\right)^m Lb \tag{25}$$

For the specific cases mentioned before one has

(*a*) *Pure bending* ($k = \infty$)

$$B_b = L\left(\frac{\sigma_b - \sigma_u}{\sigma_0}\right)^m \left[\frac{h}{m+1}\left(1 - \frac{\sigma_u}{\sigma_b}\right) + b\right] \tag{26}$$

(*b*) *Fourth-point loading* ($k = 4$)

$$B_b = \frac{L}{m+1}\left(1 - \frac{\sigma_u}{\sigma_b}\right)\left(\frac{\sigma_b - \sigma_u}{\sigma_0}\right)^m \left(\frac{h}{2} + \frac{h}{2}\sum + \frac{b}{2}\right) + \frac{2hL}{4(m+1)\sigma_b\sigma_0{}^m}(-\sigma_u)^{m+1} \ln \frac{h}{2y_u} + \frac{1}{2}\left(\frac{\sigma_b - \sigma_u}{\sigma_0}\right)^m Lb \tag{27}$$

(*c*) *Third-point loading* ($k = 3$)

$$B_b = \frac{L}{m+1}\left(1 - \frac{\sigma_u}{\sigma_b}\right)\left(\frac{\sigma_b - \sigma_u}{\sigma_0}\right)^m \left(\frac{h}{3} + \frac{2h}{3}\sum + \frac{2b}{3}\right) + \frac{1}{3}\left(\frac{\sigma_b - \sigma_u}{\sigma_0}\right)^m Lb + \frac{2hL}{3(m+1)\sigma_b\sigma_0{}^m}(-\sigma_u)^{m+1} \ln \frac{h}{2y_u} \tag{28}$$

(*d*) *Three-point loading (center-point loading;* $k = 2$)

$$B_b = \frac{L}{m+1}\left(1 - \frac{\sigma_u}{\sigma_b}\right)\left(\frac{\sigma_b - \sigma_u}{\sigma_0}\right)^m (h\Sigma + b) + \frac{2hL}{2(m+1)\sigma_b\sigma_0{}^m}(-\sigma_u)^{m+1} \ln \frac{h}{2y_u} \tag{29}$$

When $\sigma_u = 0$, both equations (24) and (25) reduce to

$$B_b = L\left(\frac{\sigma_b}{\sigma_0}\right)^m \left(\frac{h}{m+1} + b\right)\frac{k(m+1) - 2m}{k(m+1)} \tag{30}$$

For the specific values of k considered in the foregoing, equation (30) yields

(*a*) *Pure bending* ($k = \infty$)

$$B_b = L\left(\frac{\sigma_b}{\sigma_0}\right)^m \left(\frac{h}{m+1} + b\right) \tag{31}$$

(*b*) *Fourth-point loading* ($k = 4$)

$$B_b = L\left(\frac{\sigma_b}{\sigma_0}\right)^m \left(\frac{h}{m+1} + b\right)\frac{m+2}{2(m+1)} \tag{32}$$

(*c*) *Third-point loading* ($k = 3$)

$$B_b = L\left(\frac{\sigma_b}{\sigma_0}\right)^m \left(\frac{h}{m+1} + b\right)\frac{m+3}{3(m+1)} \tag{33}$$

(*d*) *Three-point loading (center-point loading;* $k = 2$)

$$B_b = L\left(\frac{\sigma_b}{\sigma_0}\right)^m \left(\frac{h}{m+1} + b\right)\frac{1}{m+1} \tag{34}$$

Equation (30) contains the same loading factor K as equation (18). In the case of surface-distributed flaws the loading factor can be redefined and extended to include the effect of the width-to-depth ratio of the beam. Thus, equation (30) can be rewritten as

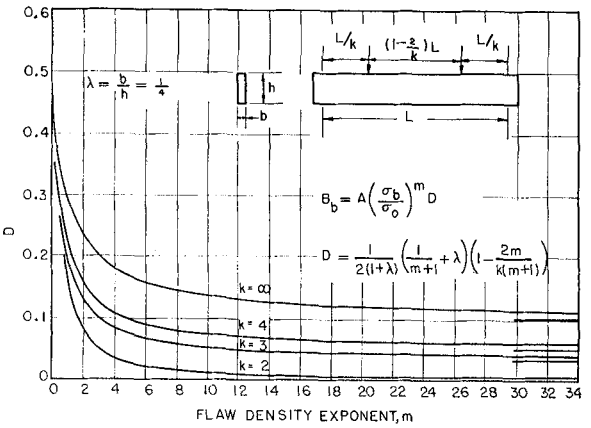

Fig. 3. Loading-shape factor D vs. flaw density exponent m for material governed by surface flaw distribution; $b/h = 1/4$.

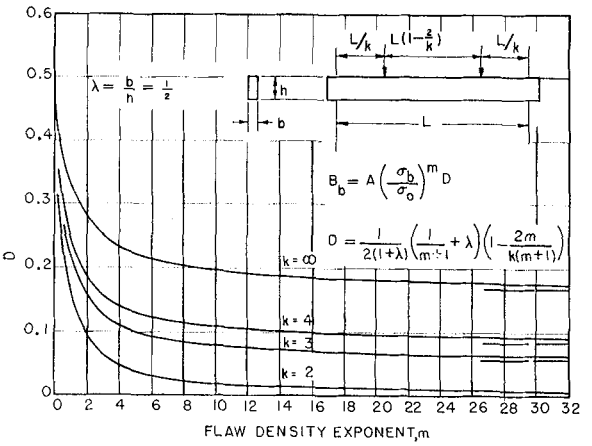

Fig. 4. Loading-shape factor D vs. flaw density exponent m for material governed by surface flaw distribution; $b/h = 1/2$.

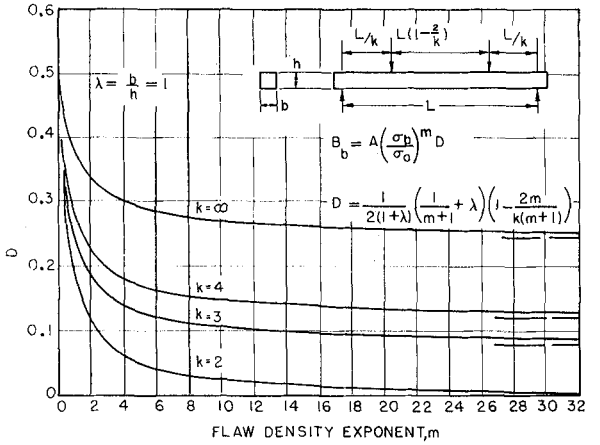

Fig. 5. Loading-shape factor D vs. flaw density exponent m for material governed by surface flaw distribution; $b/h = 1$.

$$B_b = A \left(\frac{\sigma_b}{\sigma_0}\right)^m D \tag{35}$$

where A is the surface area of the beam and

$$D = \frac{1}{2(1+\lambda)} \left(\frac{1}{m+1} + \lambda\right) \frac{k(m+1) - 2m}{k(m+1)} \tag{36}$$

with $\lambda = b/h$

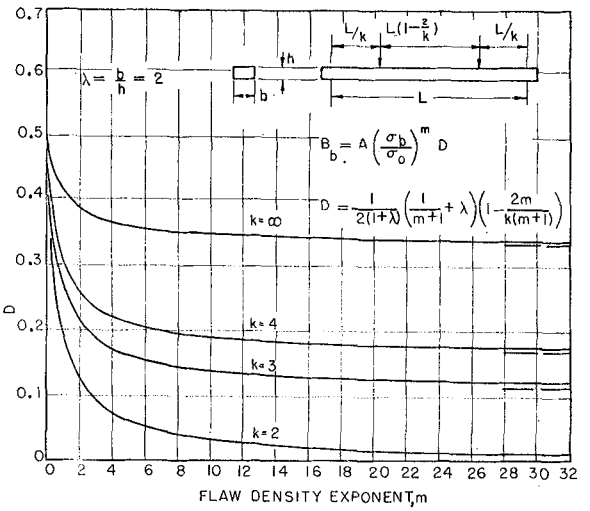

Fig. 6. Loading-shape factor D vs. flaw density exponent m for material governed by surface flaw distribution; $b/h = 2$.

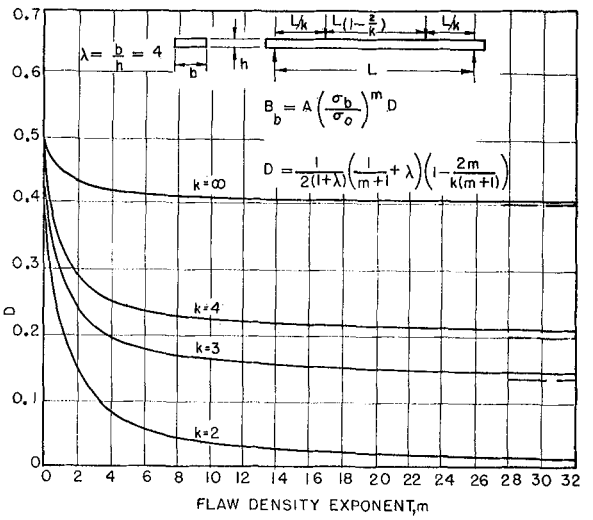

Fig. 7. Loading-shape factor D vs. flaw density exponent m for material governed by surface flaw distribution; $b/h = 4$.

The relation among the values B_b given in equations (31) through (34) is illustrated in Figs. 3 through 7 by plotting the combined loading-shape factor D versus parameter m.

IV. Relation Between Bending and Tensile Strengths

For a material governed by volumetric flaw distribution the risk of rupture in a tensile specimen is

$$B_t = V_t \left(\frac{\sigma_t - \sigma_u}{\sigma_0}\right)^m \tag{37}$$

where V_t is the volume of the specimen,

whereas for a prismatic specimen under pure bending the risk of rupture was given by equation (14).

To compare mean failure stresses, the risks of rupture given in the foregoing must be substituted in equation (3) in order to compute σ_m for the two cases. This is quite involved, however, for the case of pure bending since equation (3) cannot be solved in closed-form expression. Instead, median failure stresses (or any stresses of a given probability of fracture for that matter) are easily compared by equating instead

the risks of rupture corresponding to the different loading conditions

$$V_t\left(\frac{\sigma_t - \sigma_u}{\sigma_0}\right)^m = \frac{V_b}{2(m+1)}\left(1 - \frac{\sigma_u}{\sigma_b}\right)\left(\frac{\sigma_b - \sigma_u}{\sigma_0}\right)^m$$

from which

$$\frac{\sigma_t}{\sigma_b} = \left[\frac{1}{2(m+1)}\frac{V_b}{V_t}\right]^{1/m}\left(1 - \frac{\sigma_u}{\sigma_b}\right)^{1+\frac{1}{m}} + \frac{\sigma_u}{\sigma_b} \qquad (38)$$

For $\sigma_u = 0$ this expression reduces to

$$\frac{\sigma_t}{\sigma_b} = \left[\frac{1}{2(m+1)}\frac{V_b}{V_t}\right]^{1/m} \qquad (39)$$

In this case the relation between median stresses is the same as that between mean stresses, as can be shown easily. In the case of a classical material ($m = \infty$), equation (38) yields $\sigma_t = \sigma_b = \sigma_u$.

For a material governed by surface flaw distribution the risk of rupture in a tensile specimen of rectangular cross section ($b \times h$) is

$$B_t = 2L(b+h)\left(\frac{\sigma_t - \sigma_u}{\sigma_0}\right)^m \qquad (40)$$

as compared with equation (26) which gives the risk of rupture under conditions of pure bending.

Equating risks of rupture one obtains the following relation:

$$\frac{\sigma_t}{\sigma_b} = \left[\frac{(m+1)\frac{b}{h} + 1 - \frac{\sigma_u}{\sigma_b}}{2(m+1)\left(1 + \frac{b}{h}\right)}\right]^{1/m}\left(1 - \frac{\sigma_u}{\sigma_b}\right) + \frac{\sigma_u}{\sigma_b} \qquad (41)$$

which, for $\sigma_u = 0$, reduces to

$$\frac{\sigma_t}{\sigma_b} = \left[\frac{(m+1)\frac{b}{h} + 1}{2(m+1)\left(1 + \frac{b}{h}\right)}\right]^{1/m} \qquad (42)$$

V. Analytical Determination of Material Parameters

Experimental determinations of material parameters generally call for testing a number of simple calibration specimens and passing a curve through the data points presented in a plot showing the probability of fracture versus the failure stress. Given a theory, such as the Weibull theory, an expression for the probability of fracture can be obtained which is a function of specimen geometry and material parameters to achieve a best fit. The objective is, then, to find those values of the material parameters which make the theoretical curve fit the experimental points best. A suitable criterion for this purpose is the minimization of the sum of the mean squares differences. This method, developed in the following, is applicable to materials governed either by volumetric or surface flaw distribution.

(1) Material Governed by Volumetric Flaw Distribution

The probability of fracture at the stress σ_n is

$$S_n = 1 - e^{-B_n} \qquad (43)$$

Combining this with the expression for the risk of rupture given in equation (14), there results

$$y_n = \ln\ln\frac{1}{1 - S_n} = \ln B_n = \ln\frac{V}{2} - \ln(m+1) + (m+1)\ln(\sigma_n - \sigma_u) - \ln\sigma_n - m\ln\sigma_0 \qquad (44)$$

The corresponding (estimated) value of this function of probability of fracture obtained experimentally is

$$Y_n = \ln\ln\frac{N+1}{N+1-n} \qquad (45)$$

where

N = total number of specimens tested.
n = serial number of specimen (when specimens are ordered according to ascending values of the fracture stress σ_n).

The least squares method requires that for a best fit

$$\sum_{n=1}^{N}(Y_n - y_n)^2 = \text{minimum} \qquad (46)$$

The necessary conditions for the existence of this minimum are

$$\sum_{n=1}^{N}(Y_n - y_n)\frac{\partial y_n}{\partial \sigma_u} = 0$$
$$\sum_{n=1}^{N}(Y_n - y_n)\frac{\partial y_n}{\partial \sigma_0} = 0 \qquad (47)$$
$$\sum_{n=1}^{N}(Y_n - y_n)\frac{\partial y_n}{\partial m} = 0$$

which reduce to

$$\sum_{n=1}^{N}\left(\ln\ln\frac{N+1}{N+1-n} - \ln B_n\right)\frac{1}{\sigma_n - \sigma_u} = 0$$
$$\sum_{n=1}^{N}\left(\ln\ln\frac{N+1}{N+1-n} - \ln B_n\right) = 0 \qquad (48)$$
$$\sum_{n=1}^{N}\left(\ln\ln\frac{N+1}{N+1-n} - \ln B_n\right)\ln\left(\frac{\sigma_n - \sigma_u}{\sigma_0}\right) = 0$$

(2) Material Governed by Surface Flaw Distribution

Using in this case the expression for the risk of rupture given by equation (26) the theoretical relation between the probability of fracture, S_n, and the corresponding failure stress, σ_n, becomes

$$y_n = \ln\ln\frac{1}{1 - S_n} = \ln B_n = \ln L + m\ln(\sigma_n - \sigma_u) - m\ln\sigma_0 + \ln\left[\frac{h}{(m+1)}\left(1 - \frac{\sigma_u}{\sigma_n}\right) + b\right] \qquad (49)$$

Application of the least squares method again leads to equations (47), which in the present case reduce to

$$\sum_{n=1}^{N}\left(\ln\ln\frac{N+1}{N+1-n} - \ln B_n\right)\times\left\{\frac{m}{\sigma_n - \sigma_u} + \frac{h}{\left[\frac{h}{m+1}\left(1 - \frac{\sigma_u}{\sigma_n}\right) + b\right](m+1)\sigma_n}\right\} = 0$$
$$\sum_{n=1}^{N}\left(\ln\ln\frac{N+1}{N+1-n} - \ln B_n\right) = 0 \qquad (50)$$
$$\sum_{n=1}^{N}\left(\ln\ln\frac{N+1}{N+1-n} - \ln B_n\right)\times\left\{\frac{h\left(1 - \frac{\sigma_u}{\sigma_n}\right)}{\left[\frac{h}{m+1}\left(1 - \frac{\sigma_u}{\sigma_n}\right) + b\right](m+1)^2} - \ln\left(\frac{\sigma_n - \sigma_u}{\sigma_0}\right)\right\} = 0$$

Equations (48) and (50), depending on the type of material, are solved for the three material parameters σ_u, σ_0, and m. They are too involved for a conventional solution to be attempted and a computer solution is required.

VI. Experimental Work

The material used for the experimental evaluation of the method described in the foregoing was Columbia Resin (CR-39), an amorphous brittle polymer. Thirty-six CR-39 specimens 0.4 by 0.4 by 4 in. were cut from a sheet 1/2 in.

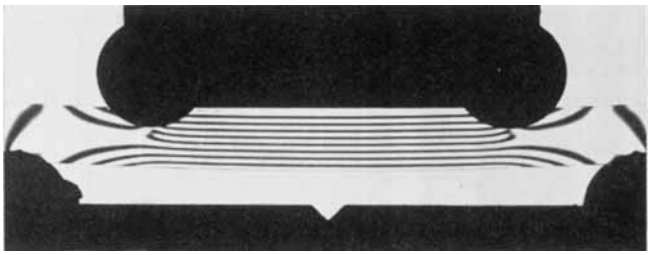

Fig. 8. Isochromatic fringe pattern n CR–39 specimen under four-point loading.

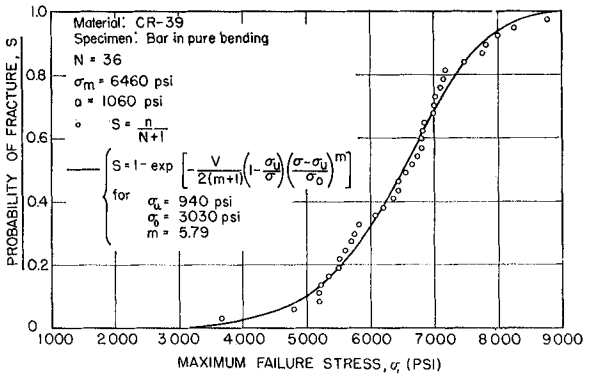

Fig. 9. Comparison of experimental values with theoretical cumulative distribution curve of best fit.

thick; all the surfaces of each specimen had a uniformly machined finish. These specimens were tested under four-point loading with a gage length of 2 in. subjected to pure bending and a distance of 3/4 in. between loads and supports. The existence of pure bending between the two middle loads is illustrated by the isochromatic fringe pattern of Fig. 8, obtained on one such specimen under four-point loading. The specimens were tested in an Instron model TT testing machine with a crosshead speed of 0.5 in. per minute. A load-versus-crosshead deflection record was obtained in each case, and no deviation from linearity was noted. Although this fact does not preclude localized nonlinear deformation, the data were analyzed on the basis of linear elastic behavior to failure. The following results were obtained:

Mean failure stress: $\sigma_m = 6460$ psi
Standard deviation: $a = 1060$ psi
Variance: $a^2 = 1{,}123{,}600$ (psi)^2
Coefficient of variation: $v = 16.41\%$
Highest failure stress: $\sigma_{\text{high}} = 8780$ psi
Lowest failure stress: $\sigma_{\text{low}} = 3670$ psi

A volumetric flaw distribution was assumed, and equations (48) were solved by the computer for the desired material parameters. The following values were obtained:

$\sigma_u = 940$ psi
$\sigma_0 = 3030$ psi
$m = 5.79$

The theoretical cumulative distribution curve of equation (43) for the values of the parameters found in the foregoing was plotted in Fig. 9 along with the experimental points based on the relation

$$S_n = \frac{n}{N+1}$$

It is seen that the fit is very satisfactory. It should be remarked, however, that the nature of the fitting criterion used (minimization of least squares) does not necessarily guarantee a best fit in other respects; e.g., the derivative of the cumulative distribution function which provides the probability density function may not show an equally satisfactory correlation.

VII. Discussion

Equation (12) shows that, for materials whose fracture is governed by a volumetric flaw distribution, the only specimen dimension entering the expression for the risk of rupture is the total volume V. For a fixed value of the parameter k, variations in length, width, or depth of specimen which leave its volume unaffected will not affect the risk of rupture; the risk of rupture therefore is independent of (transversal) stress gradient.

The dependence of the risk of rupture on specimen dimensions is more complicated for a material governed by a surface flaw distribution. For a given material, σ_0, σ_u, and m are constants. If one is interested solely in the effect of depth and width on the risk of rupture, h and b should be regarded as being the only variables, whereas the length L and extreme fiber stress σ_b should be kept constant. Then, the risk of rupture for a pure bending specimen, as given by equation (26), remains constant provided b and L satisfy the relation

$$\frac{h}{m+1}\left(1 - \frac{\sigma_u}{\sigma_b}\right) + b = \text{constant}$$

Substituting $h = 2\sigma_b/g$, where g is the stress gradient, results in

$$\frac{2\sigma_b}{g(m+1)}\left(1 - \frac{\sigma_u}{\sigma_b}\right) + b = \text{constant}$$

or

$$\frac{C_1}{g} + b = C \tag{51}$$

where

$C_1 = \frac{2}{m+1}(\sigma_b - \sigma_u)$.
C = constant.

From equation (51) it follows that it is possible to vary the stress gradient without affecting the risk of rupture, provided the width b varies in such a manner that equation (51) is satisfied, with appropriate reference to the strength of the material, σ_b.

For purposes of determining material parameters any type of bending test is suitable if $\sigma_u = 0$. If $\sigma_u \neq 0$, material parameters can be uniquely determined from a tensile test or a pure bending test. This means that for four-point loading the loads should be as close to the supports as practicable, and yet without incurring the risk of causing shear failures to develop next to the support points. In general, it is possible to apply the equations for pure bending to the results obtained from tests of beams subjected to symmetric four-point loading if only fractures occurring in the portion of the beam under constant bending moment are regarded as being valid. Tests resulting in fracture outside the gage length of interest (between supports and loading points) would be discarded from the statistical analysis.

The conventional trial-and-error method for the determination of parameters is suitable for tensile, torsion, and pure bending specimens in the case of volume-distributed flaws and only for tensile and torsion specimens in the case of surface-distributed flaws. The method as it is usually applied is not entirely free of subjectivity. The analytical method described here is more general and is especially advantageous in the case of surface-distributed flaws. Its successful application was clearly demonstrated in the case of CR–39.

VIII. Conclusion

In the statistical failure theories developed to date it is assumed implicitly that the probability of fracture is governed

by the tensile normal stresses existing in an element and is independent of the intensity of shear stresses existing in any part of a body. The overall fracture probability of a piece is then obtained by summing up the individual failure probabilities of infinitesimal components composing the body, this result remaining independent of the stress gradient accompanying the internal stress distribution.

The validity of this hypothesis has never been examined. The present investigation, therefore, was aimed at evolving a carefully conceived approach for investigating whether or not the existence of stress gradients had an independent influence on the fracture characteristics of brittle ceramic substances.

In this paper the results of the theoretical part of the study are presented. The Weibull theory was adopted as the basis of characterization of the probabilistic fracture behavior of brittle substances. The symmetrically loaded beam under four-point bending was selected as the principal subject of analysis, both because it represents one of the easiest shapes for analysis and experiments and because it is one of the geometrical configurations that can yield conclusive proof regarding the influence of stress gradients through the simple expedient of changing the proportions but retaining the area of the rectangular cross section.

A theoretical treatment was developed for the completely general case of an arbitrary positioning of the two symmetrically disposed loads on the beam, for the case of a nonintegral value of m and a nonvanishing value of σ_u. Solutions of this nature were obtained for both of the broad cases possible with the Weibull theory; that is, the cases where significant flaws are uniformly dispersed volumetrically or confined to the surface. Substantial simplifications in the resulting expressions are shown to be possible (1) if m is an integer and (2) if σ_u has a vanishing value. The special cases of pure bending and fourth-point, third-point, and center-point loading were derived, the first and the last of these representing the limiting cases of the general solution.

Because no completely satisfactory treatment of a most reliable fit of the Weibull probability density curve to experimental data exists in the current literature (for $\sigma_u \neq 0$), an analytical method of obtaining the best fit of a theoretical curve to a set of test points is presented, following the analytical derivations for the effect of nonuniform stresses. The process producing this best fit is based on a minimization of the sum of the mean squares of theoretical and experimental data, which then yield the most reliable values of three parameters descriptive of the Weibull distribution. The methodology thus developed is illustrated by applying it to a set of test data obtained with specimens of CR-39, a brittle polymeric material.

Experimental work in support of the analytical studies presented here was completed recently and the results were presented in another paper.[1]

Acknowledgment

Appreciation is due to J. B. Blandford and W. G. Ramke for their helpful suggestions during the course of this study.

Flux Growth of Chrysoberyl and Alexandrite

by E. F. FARRELL and J. H. FANG

Laboratory for Insulation Research, Department of Electrical Engineering, Massachusetts Institute of Technology, Cambridge, Massachusetts

Chrysoberyl (Al_2BeO_4) and alexandrite (Al_2BeO_4:Cr) crystals have been grown successfully by the flux-melt method in lengths from 0.1 to 10.0 mm. A satisfactory composition for chrysoberyl is PbO 66.6, Al_2O_3 16.7, and BeO 16.7 mole %; for alexandrite, Li_2MoO_4 40.4, MoO_3 50.6, Al_2O_3:Cr 4.5, and BeO 4.5 mole %. Morphological characteristics of the crystals produced are described.

I. Introduction

The oxygen atoms in the chrysoberyl structure are arranged in a slightly distorted hexagonal close-packed fashion[1] similar to that of the corundum structure. Furthermore, the structure has a counterpart with regard to oxygen packing, namely the cubic close-packed spinel structure. Thus its similarity to ruby and to spinel make the chrysoberyl structure an interesting host lattice into which various transition metal ions can be substituted and their optical, magnetic, and electrical properties investigated. Chrysoberyl may also be useful for solid-state maser applications. It has a characteristic spectrum exhibiting green in daylight and red by incandescent light. Since measurements of its physical properties require good-quality single crystals, a program to grow pure and doped crystals of Al_2BeO_4 was initiated. In the present paper the initial success in synthesizing single crystals of both chrysoberyl and alexandrite is reported.

II. Experimental

Early attempts to synthesize chrysoberyl have been described by Palache *et al.*[2] Since attempts to duplicate their results were unsuccessful, a series of experiments was started employing other solvents, including KF, PbO, PbO-PbF_2, V_2O_5, Li_2MoO_4, and $Li_2Mo_2O_7$. Experiments in which the first three solvents were used are also described briefly in footnote 1.

These experiments were conducted in an Alundum-tube furnace equipped with eight vertical Globars. The variable electrical power supply was equipped with a drive mechanism that allowed the cooling rate to be adjusted from 100° to 0.5°C per hour. The mixtures of component oxides and fluxes either just filled platinum crucibles (15, 50, and 100 ml) or were packed tightly. At a later stage, crucibles

Presented at a meeting of the Mineralogical Society of America, New York, N. Y., November 1963. Received October 16, 1963; revised copy received January 11, 1964.

The writers are research members, Laboratory for Insulation Research.

[1] E. F. Farrell, J. H. Fang, and R. E. Newnham, "Refinement of Chrysoberyl Structure," *Am. Mineralogist*, **48** [7-8] 804-10 (1963).

[2] Charles Palache, Harry Berman, and Clifford Frondel, Dana's System of Mineralogy, Vol. I, 7th ed., pp. 718-22. John Wiley & Sons, Inc., New York, 1944. 834 pp.; *Ceram. Abstr.*, **1953**, April, p. 74*b*.